ORIGINAL ARTICLE

Trace Gases over Land and Ocean Surfaces of China: Hotspots, Trends, and Source Contributions

Md. Arfan Ali[1,2] · Yu Wang[3] · Muhammad Bilal[4] · Mazen E. Assiri[2] · Abu Reza Md Towfiqul Islam[5,6] · Guilherme Malafaia[7,8,9] · Zhongwei Huang[1] · Alaa Mhawish[10] · M. Nazrul Islam[2] · Zhongfeng Qiu[3] · Rayees Ahmed[11] · Mansour Almazroui[12,13]

Abstract

Trace gases in the atmosphere (NO_2: nitrogen dioxide; SO_2: sulfur dioxide) have a major impact on both local and global air quality, human health, climate and ecological conditions. Therefore, the present study investigated 16 years (2005–2020) of Ozone Monitoring Instrument (OMI) based NO_2 and SO_2 in Dobson unit (DU) spatiotemporal distributions and variability, SO_2/NO_2 ratio, trends, and potential source contribution function (PSCF) across ocean and land areas of Jiangsu Province, China. Results demonstrated higher NO_2 and SO_2 concentrations (DU) over land (NO_2: 0.58 and SO_2: 0.56) than in the ocean (NO_2: 0.30 and SO_2: 0.38) due to more concentrated anthropogenic activities on land surfaces. There were significant seasonal variations in NO_2 and SO_2, with winter being the highest and summer being the lowest. The SO_2/NO_2 ratio shows land and ocean pollution is caused by NO_2 and SO_2 emissions from ships and industrial processes. Furthermore, OMI-based trace gases and anthropogenic emissions showed a good correlation (NO_2 vs $NO_x = 0.626$ and SO_2 vs SO_2 emission $= 0.871$) across land surfaces than the ocean (NO_2 vs $NO_x = 0.366$). NO_2 and SO_2 levels over land surfaces decreased significantly (at a 95% confidence level) compared to the ocean on annual and seasonal scales, which is attributed to a decrease in NO_x and SO_2 emissions. Furthermore, PSCF analysis shows that local sources have a greater impact on air quality than long-distance sources over land and ocean. It is concluded from this study that Chinese air pollution control policies achieved a satisfactory improvement in Jiangsu's air quality by reducing NO_2 and SO_2. It is therefore recommended to continue or extend these policies in the future to improve China's air quality, which will benefits its citizens.

1 Introduction

Numerous environmental problems, such as air pollution, have arisen from China's fast industrialization, socioeconomic development, urbanization, and meteorological factors (Chan and Yao 2008; de Leeuw et al. 2021; Wei et al. 2023). Aerosol and gaseous pollutants (e.g., aerosol optical depth: AOD, particulate matters, Ozone, nitrogen dioxide: NO_2, sulfur dioxide: SO_2) are the leading causes of air pollution (Wang et al. 2021b). Two atmospheric trace gases, NO_2 and SO_2, play a significant role in chemical reactions. For example, by reacting with hydroxyl radicals (OH), NO_2 produces aerosols and acid rain through an oxidizing process in the atmosphere, which are dangerous to both the atmospheric environment (reducing vegetation and forest, corroding buildings, and contributing to heating worldwide) and health problems (asthma, colds, coughs, flu, bronchitis, and cancer) (Lelieveld et al. 2002; Lelieveld and Dentener 2000; Seinfeld and Pandis 2006). Both anthropogenic activities (e.g., burning of fossil fuel and biomass, electric- and coal-based power plants) and natural sources (volcanoes, oceans, biological decay, and lightning) produce the emission of nitrogen oxides (NO_x) (Lee et al. 1997). Among China's NO2 emissions in 2010, 39% came from industry, 32% from power plants, 25% from traffic, and 4% from residential activities (Li et al. 2017a, b). Furthermore, SO_2 contributes to producing sulfate aerosols and acid rain, which negatively affect human health (e.g., breathing problems for asthmatic children and adults, cardiovascular or chronic lung disease)

Md. Arfan Ali, Yu Wang and Muhammad Bilal with equal contributions.

Extended author information available on the last page of the article

(Miller 2005), as well as the atmospheric environment (climate and building corrosion) (Hutchinson and Whitby 1977; Pope and Dockery 2006). SO_2 comes from a variety of natural (e.g., volcanoes, fires, and phytoplankton) and anthropogenic sources (e.g., burning of high-sulfur coals and heating oils in power plants, industrial boilers, and metal smelting) (Jain et al. 2016). NO_2 and SO_2 emissions from ships also adversely affect coastal and inland air quality (within a hundred kilometers of the emission sources) (Lv et al. 2018). In addition, the effects of NO_2 and SO_2 on air quality, the climate, human health, terrestrial acidification, and marine ecosystems (Berglen 2004; Seinfeld and Pandis 2006).

Carey et al. (2013) reported that long-term exposure to NO_2 and SO_2 could increase mortality rates. Long-term exposure to NO_2 is also accountable for the significant increase in China's respiratory and cardiovascular mortality rates (Dong et al. 2012; Tao et al. 2012). To account for the effects of NO_2 and SO_2 on human health and the atmospheric environment, several researchers around the globe have investigated the characteristics of these two gaseous pollutants using both ground and satellite observations (Bilal et al. 2021; Hilboll et al. 2013; Krotkov et al. 2016; Lin and McElroy 2011; Zhang et al. 2017a, b; Zheng et al. 2018a, b).

Ground-based observations stations can present accurate and reliable scenarios of gaseous pollutants, providing details of their temporal distributions and their consequences on the climate and human health (Zhang et al. 2017a, b; Zheng et al. 2018a, b). However, the ground-based stations are unevenly and sparsely distributed and thus can fail to identify NO_2 and SO_2 pollution hotspots at fine spatial scales (Wang et al. 2021b). Satellite-based observations provide near-real-time (NRT) long-term data of gaseous pollutants (e.g., NO_2 and SO_2) with global coverage at different spatial resolutions and thus, can overcome the limitations of ground-based measurements. In addition, satellite-based observations allow long-distance NO_2 and SO_2 transportation assessment (Lu et al. 2013; Wang et al. 2011) and identify contributions from different sources (Zhang et al. 2008). Several satellite-based sensors, namely the Global Ozone Monitoring Experiment (GOME) instrument (Burrows et al. 1999; Eisinger and Burrows 1998), the Scanning Imaging Absorption spectrometer for Atmospheric CHartographY (SCIAMACHY) (Bovensmann et al. 1999), GOME-2 (Callies et al. 2004; Munro et al. 2016), the Ozone Monitoring Instrument (OMI) (Levelt et al. 2006a, b), and the TROPOspheric Monitoring Instrument (TROPOMI) (Veefkind et al. 2012), have been built and launched to acquire accurate evidence about atmospheric gaseous pollutants. However, OMI, in particular, provides long-term observations of the atmospheric gaseous pollutants at high spatial (13×24 km, at nadir) with daily global coverage (Krotkov et al. 2016; Levelt et al. 2018). OMI-based measurements have been widely used for monitoring air quality by detecting aerosols, NO_2,

SO_2, and formaldehyde (HCHO) and detecting Ozone (O3), volcanic emission, and solar radiation. Globally, OMI-based NO_2 showed a good correlation (r=0.80–0.90) with ground-based measurements (Celarier et al. 2008). A study over the United States also reported a good correlation between satellite (GOME and OMI) and ground-based NO_2 measurements (Penn and Holloway 2020). Consequently, many researchers have used satellite observations worldwide to investigate NO_2 and SO_2 pollution. For example, Krotkov et al. (2016) investigated changes in OMI-based NO_2 and SO_2 pollution over the United States, Asia, and Europe from 2005 to 2015 and reported decreasing and increasing trends in NO_2 and SO_2. Jion et al. (2023) reported increasing trends in NO2 and SO2 pollution across Asian countries due to the excess burning of biomass and fossil fuel, and power plants. In addition, Lamsal et al. (2015) evaluated the trends in OMI-based tropospheric NO_2 vertical column density (VCD) against ground-based measurements over the United States. ul-Haq et al. (2015) studied the spatiotemporal distributions and variations of OMI-based NO_2 and its trend from 2004 to 2015 over South Asian countries. Bilal et al. (2021) have characterized polluted cities of Pakistan based on long-term (2004–2019) NO_2 and SO_2 observations from OMI.

Some previous studies also validated and analyzed spatiotemporal distributions and trends of OMI-based NO_2 and SO_2 over mainland China (Cui et al. 2016; Li et al. 2017a, b; Li et al. 2010; Liu et al. 2017, 2016; van der A et al. 2017; Wang et al. 2021b, 2017; Wei et al. 2023; Zhai et al. 2023; Zhang et al. 2017a, b; Zheng et al. 2018a, b). However, none of them attempted to analyze spatiotemporal distributions and variability of OMI-based NO_2 and SO_2 with their trends over the ocean. Only a single study has investigated NO_2, SO_2, and HCHO over the East China Sea using ship-based MAX-DOAS and satellite observations (OMI and Ozone Mapping and Profiler Suite (OMPS)) (Tan et al. 2018). Generally, in marine environments, the concentrations of trace gases are very low because no emission sources exist there, except for some maritime transport and natural sources. Schreier et al. (2015) reported low NO_2 VCD ($< 0.5 \times 10^{15}$ molec/cm^2) in the marine environment of the South China and Sulu seas. In addition, they found boundary layer values of NO_2 less than 100 pptv and 30 pptv in the open and clean tropical marine environment of the South China and Sulu seas, respectively. The time-series magnitudes of SO_2 concentrations were consistent with NO_2 in these areas. Takashima et al. (2012) also reported low NO_2 concentrations (~0.2 ppbv) over the western Pacific and Indian oceans. However, concentrations of these pollutants were high close to the shore due to the operations of busy ports and vessels (Schreier et al. 2015; Takashima et al. 2012). These pollutants significantly affect local and regional air pollution in both inland and offshore areas of the Yangtze River Delta (YRD) region (Fan et al. 2016; Zhang et al. 2017a, b). In

recent years they have also affected the ecology and environment of the continental YRD region, including the coast and land areas of Jiangsu province (Chen et al. 2017; Song et al. 2017). Therefore, it is crucial to identify NO_2 and SO_2 pollution hotspots and sources over both the ocean and land regions of Jiangsu Province. This is the first study to identify the pollution hotspots using long-term (2005–2020) OMI-based NO_2 and SO_2 data and their sources over the ocean and land in Jiangsu province, China. The present study is designed based on the following three main objectives: (1) to analyze long-term spatiotemporal distributions and variations of OMI-based NO_2 and SO_2, their ratio, and trends, (2) to measure the contributions of anthropogenic emissions (NO_x and SO_2) to total NO_2 and SO_2 concentration changes, and (3) to identify the potential source areas using PSCF analysis. This study provides a better understanding of local emission sources over the land and ocean surfaces of Jiangsu, China as a result of the interaction with atmospheric gaseous pollutants in the atmosphere.

2 Study Area

The land and ocean parts of Jiangsu Province cover between 30° 5′–35° N and 116° 5′–126° 3′ E (Fig. 1). Jiangsu Province is an economically developed province in eastern China, having dense metropolises and large rural areas. Crop residue burning, high traffic volumes, industrial production, and urban construction activities in the province cause significant air pollution (Wang et al. 2021a). The province is

between the YRD and the Beijing-Tianjin-Hebei (BTH) regions, where air pollution frequently occurs. The coastal waters of the YRD regions (e.g., Jiangsu, Shanghai, and Zhejiang) are the busiest sea area of the East China Sea (ECS), known as the three key Ship Emission Control Zones (ECZs) of China (see Fig. 1). In addition, the continental YRD region is a developed industrial city cluster of China or even the world. More than 15 large ports exist in the YRD coastal port cluster, with a flourishing shipping industry that releases SO_2, NO_2, and $PM_{2.5}$ in the atmosphere.

3 Materials and Methods

3.1 OMI Data

The OMI, a near-polar orbiting sensor of the Aura satellite, crosses the equator at 13:45 (local time), hovering over 705 km from the earth's surface. It was deployed on 15th 2004 July by NASA with the cooperation of Finland, the United Kingdom, and the Netherlands. This sensor uses 250–500 nm wavelengths to measure the reflected solar radiation daily at a spatial resolution of 13×25 km at the nadir. OMI UV spectral measurements utilize several algorithms to retrieve total and tropospheric column densities of trace gases such as NO_2 and SO_2 (Krotkov et al. 2016; Carn et al. 2017). In the present study, OMI version 3 (V3) level-3 (L3) daily total column NO_2 (OMNO2d; cloud-screened: cloud fraction < 30%) and SO_2 (cloud radiance
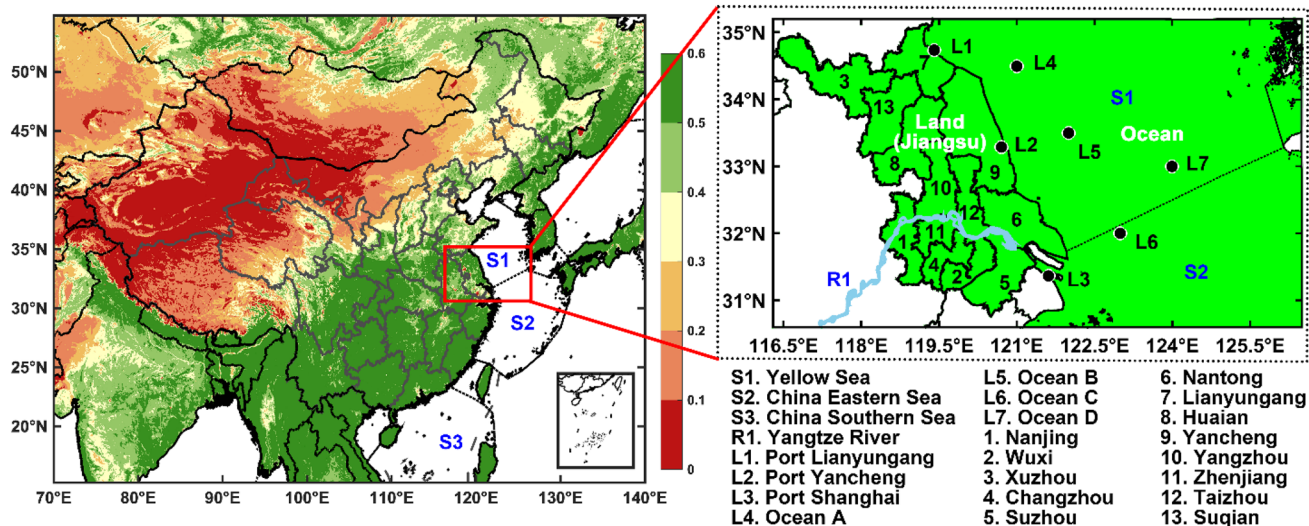
Fig. 1 Map of the study area, including China's ocean and land (Jiangsu Province) surface. The background image reveals the multi-year (2005–2020) averages of MODIS NDVI, with arid surfaces (NDVI < 0.2), lighter or sparse vegetation (0.2 < NDVI < 0.4), moderate vegetation (0.4 < NDVI < 0.5), and dark vegetation (NDVI > 0.5).

Sea boundary is taken from Glaciology and Geocryology Data Center, National Earth System Science Data Sharing Infrastructure, National Science & Technology Infrastructure of China (http://westdc.geodata.cn/index.htm)

fraction < 0.2, OMSO2e) products with a spatial resolution of $0.25° \times 0.25°$ were used.

Furthemore, OMI-based NO_x and SO_2 emissions were used in this study to clearly understand anthropogenic emission scenarios. This study obtained a satellite-based NOx emission dataset from the DECSO (Daily Emission Constrained by Satellite Observations) algorithm. DECSO algorithm was developed to estimate NO_x emissions with a spatial resolution of $0.25° \times 0.25°$ over East Asia, West Asia, South Africa, and India (Mijling and van der A, 2012). This algorithm has been significantly upgraded and validated over South Asia (Ding et al. 2018, 2017b, 2017a). The tropospheric NO_2 column-integrated values were calculated from OMI-based NO_2 concentrations using the QA4ECV algorithm (quality assurance for the essential climate variables) (Boersma et al. 2018) and then used as input to the DECSO algorithm for estimating NO_x emissions. More details can be found in Mijling and van der A (2012) and Ding et al. (2017b). Furthermore, SO_2 emissions were estimated by combining OMI-based measurements with the Multi-resolution Emissions Inventory for China (MEIC) inventory. More details can be found in Theys et al. (2015) and van der A et al. (2017). Anthropogenic NO_x and SO_2 emissions data are accessible through the TEMIS (Tropospheric Emission Monitoring Internet Service) portal.

3.2 Methodology for NO_2 and SO_2

Several methods were applied to detect NO_2 and SO_2 pollution hotspots and identify their potential sources over ocean and land territories:

- An analysis of long-term annual and seasonal averages for the OMI-based total columns of NO_2 and SO_2 was conducted over the entire study area. Furthermore, the shapefile was used to extract area averages for Jiangsu Province's coastal and land areas for seasonal and annual analysis.
- A frequency distribution was used to visualize the variability (lows and highs) of NO_2 and SO_2 concentrations over land and ocean surfaces in Jiangsu Province, China.
- A SO_2/NO_2 ratio was used in order to identify the sources of air pollutants over land and ocean, regardless of whether they originated from mobile sources (traffic emissions) or from point sources (industrial activities). A high value of the SO_2/NO_2 ratio (> 0.60) indicates significant contributions from industrial activities over land (Wang et al. 2021b), while the SO_2/NO_2 ratio > 1.5 reflects the emission of high-sulfur fuel content from ships across the ocean (Cheng et al. 2019b).
- The Mann-Kendal (MK) test (Kendall 1975; Mann 1945) (Mann 1945; Kendall 1975), associated with the Theil-Sen's slope (Sen 1968; Theil 1992), was used to calculate

trends of NO_2 and SO_2 across ocean and land territories for the period of 2005–2020. The significance of NO_2 and SO_2 trends was calculated using a two-tailed test at a 95% confidence level. More details about the methods can be found in Wang et al. (2021a, b).

- The NOAA (National Oceanic and Atmospheric Administration) HYSPLIT (Hybrid Single-Particle Lagrangian Integrated Trajectory) model (Stein et al. 2015) was used to calculate the source of air masses (Fleming et al. 2012). This is a complete chemical transformation, dispersion, and transport model. The NOAA HYSPLIT model was combined with PSCF to detect the potential sources of NO_2 and SO_2 concentrations that influence the air quality of ocean and land territories in China. The MeteoInfo TrajStat and HYSPLIT (Wang et al. 2009) were used to compute back trajectories and identify sources of NO_2 and SO_2 concentrations across China. This method was also used in recently published papers in China and Asian countries (Ali et al. 2023; Bilal et al. 2021; Wang et al. 2021b). 72-h back trajectories at 500 m above ground level were computed for every hour at seasonal scales from 2005 to 2020 using meteorological data from GDAS (the Global Data Assimilation System) with a spatial resolution of $1° \times 1°$. The PSCF analysis used OMI-based daily NO_2 and SO_2 concentrations over a grid with a resolution of 0.5°. The PSCF value was calculated based on the assumption that the trajectory endpoint is located within a grid cell (i, j), and the trajectory was assumed to collect pollutants emitted from different pocket emission sources within that cell (i, j). The PSCF value can be explained as a conditional probability that defines the potential contributions of a grid cell to the high NO_2 and SO_2 loadings at the receptor sites. The value of PSCF for the ij[th] grid cell is calculated based on the following Eq. (2):

$$PSCF = \frac{m_{ij}}{n_{ij}} \tag{1}$$

where n_{ij} is the number of endpoints that fall or pass through the ijth cell, and m_{ij} defines the number of endpoints in the ijth cell having a concentration higher than an arbitrarily set criterion of the 75 percentile. For NO_2 and SO_2, the thresholds were 0.498 (DU) and 0.577 (DU), respectively. To reduce the uncertainty of PSCF which resulted from small n_{ij}, an arbitrary weight function (Wi,j) is multiplied into the PSCF (Eq. 2):

$$W_{i,j} = \begin{cases} if\, n_{ij} > 3\bar{n} \to 1.00 \\ if\, 1.5\bar{n} < n_{ij} \leq 3\bar{n} \to 0.70 \\ if\, \bar{n} < n_{ij} \leq 1.5\bar{n} \to 0.42 \\ if\, n_{ij} \leq \bar{n} \to 0.15 \end{cases} \tag{2}$$

here, n = average number of endpoints, which is calculated for each cell that has at least one endpoint. Hence, the Weighted PSCF (WPSCF) is computed using Eq. (3):

$$WPSCF = W_{i,j} \times PSCF(i,j) \tag{3}$$

4 Results and Discussion

4.1 *Spatial Distributions of OMI NO$_2$ and SO$_2$*

The annual and seasonal spatial distributions of OMI NO$_2$ and SO$_2$ across ocean and land surfaces of Jiangsu Province during 2005–2020 (Fig. 2). The results show higher seasonal and annual of NO$_2$ and SO$_2$ across land compared to ocean surfaces (Fig. 2). In particular, the spatial distributions of mean yearly NO$_2$ and SO$_2$ were higher (> 0.40 DU) over the northern (Xuzhou, Suqian, and Lianyuang) and southern (Changzhou, Nanjing, Suzhou, Wuxi, and Zhenjiang) cities of Jiangsu province than ocean surfaces (≤ 0.40 DU). Moreover, the 16-year area average NO$_2$ and SO$_2$ were comparatively high over land (0.58 ± 0.06 for NO$_2$ and 0.56 ± 0.11 for SO$_2$) than over ocean (0.30 ± 0.03 for NO$_2$; 0.38 ± 0.06 for SO$_2$) (Table 1). The higher NO$_2$ and SO$_2$ over land could be attributed to anthropogenic activities, as reported by Wang et al. 2021b. In contrast, relatively low concentrations over the ocean are due to fewer emission sources on ocean surfaces (Tan et al. 2018). Several studies reported that ships also contribute to NO$_2$ and SO$_2$ in marine environments (Corbett et al. 1999; Endresen 2003; Eyring et al. 2010; Matthias et al. 2010). Cheng et al. (2019a) reported that the Ship Emission Control Zones of China (ECZ) in the Pearl River Delta (PRD), the Yangtse River Delta (YRD), and the Bohai Rim (Beijing–Tianjin–Hebei) are the primary source of NO$_2$ and SO$_2$ concentrations. Therefore, the Eastern and Southern China seas are hotspots of NO$_2$ and SO$_2$ concentrations (Johansson et al. 2017). The pollution level in the marine environment is higher near the coastal areas due to busy ports and ship lanes and lower in remote oceanic regions due to less maritime traffic (Eyring et al. 2010; Fan et al. 2016). Lamsal et al. (2013) reported that dense population and unsustainable anthropogenic emissions from mobile sources (e.g., traffic emissions) also contribute to high NO$_2$ pollution over land. Increased emissions of SO$_2$ over the northern cities of Jiangsu Province are mainly attributed to significant local activities (Dahiya and Myllyvirta 2019). According to Jion et al. (2023), the burning of biomass and fossil fuel, power plants, and heavy traffic in China have resulted in higher levels of NO$_2$ and SO$_2$ pollution.

Significant seasonal variations in NO$_2$ and SO$_2$ concentrations were observed across land and ocean (Fig. 2 and Table 1). For example, the 16-year area-averaged NO$_2$ and SO$_2$ were comparatively high in winter over land surfaces (0.83 ± 0.12 for NO$_2$ and 0.75 ± 0.16 for SO$_2$) than the ocean (0.44 ± 0.08 for NO$_2$; 0.50 ± 0.09 for SO$_2$) (Fig. 2 and Table 1). This is attributed mainly to stable meteorological conditions, weak photochemical conversion, and coal burning for winter room heating (Qi et al. 2012; Zhang et al. 2017a, b). In winter, the stable atmospheric conditions and low boundary layer height accumulate and slow down the NO$_2$ washing-out process in the atmosphere, resulting in high NO$_2$ in the total column (Bilal et al. 2021; Mhawish et al. 2020; Qi et al. 2012; Zhang et al. 2017a, b). In spring, the NO$_2$ (0.56 ± 0.08) and SO$_2$ (0.60 ± 0.15) were the second-highest over land than the ocean (0.29 ± 0.03 for NO$_2$; 0.44 ± 0.09 for SO$_2$) (Table 1). In summer, the NO$_2$ and SO$_2$ were lowest both over land (NO$_2 = 0.34 \pm 0.02$; SO$_2 = 0.33 \pm 0.06$) and ocean (0.20 ± 0.01 and 0.23 ± 0.03), which is attributed to the plenty of precipitation, rapid photochemical conversion, and better atmospheric diffusion (Feng et al. 2001; Qi et al. 2012). Higher NO$_2$ and SO$_2$ (0.58 ± 0.05 and 0.54 ± 0.14) over land surface compared to the ocean (0.25 ± 0.03 for NO$_2$; 0.34 ± 0.05 for SO$_2$) were also noticed in autumn (Table 1). High NO$_2$ and SO$_2$ in winter were also reported by several studies conducted over China (Meng et al. 2010; Wang et al. 2021b; Xue et al. 2020; Zhang et al. 2017a, b; Zheng et al. 2018a, b; Zheng et al. 2014).

4.2 Frequency Distributions of OMI NO$_2$ and SO$_2$

The annual and seasonal frequency distributions of daily OMI NO$_2$ and SO$_2$ over ocean and land for 2005–2020 (Fig. 3). The occurrence frequency of NO$_2$ and SO$_2$ were calculated for each 0.15 (DU) interval (Fig. 3). At annual timescale, the NO$_2$ and SO$_2$ occurrence frequencies over the ocean were highest for the 0.15–0.30 bin (e.g., NO$_2 = 65.70\%$ and SO$_2 = 36.65\%$). On the other hand, the highest NO$_2$ and SO$_2$ occurrence frequencies over land were observed for 0.30–0.45 bin (NO$_2 = 32.12\%$ and SO$_2 = 21.82\%$) (Fig. 3). The occurrence of high NO$_2$ (> 0.45 DU) was higher over land than over ocean (Occurrence frequency: land ~ 52%; ocean ~ 12%). Similarly, the occurrence of high SO$_2$ (> 0.45 DU) was also higher over land (53%) than over the ocean (25%). A previous study also reported that the land surfaces of Jiangsu Province are affected mainly by moderate (0.30–0.45 DU) NO$_2$ and SO$_2$ pollution (Wang et al. 2021b). Notably, very high NO$_2$ and SO$_2$ pollution (bin > 0.60) also affect both land (NO$_2 = 33\%$; SO$_2 = 34\%$) and ocean (NO$_2 = 7\%$; SO$_2 = 12\%$) surfaces (Fig. 3). The ship traffic density and atmospheric dispersion are the main drivers of SO$_2$ and NO$_2$ variations over ocean surfaces (Cheng et al. 2019b). Furthermore, the NO$_2$ and SO$_2$ occurrence frequencies display a marked seasonal cycle (Fig. 3). Seasonally, the winter NO$_2$ and SO$_2$ occurrence frequencies
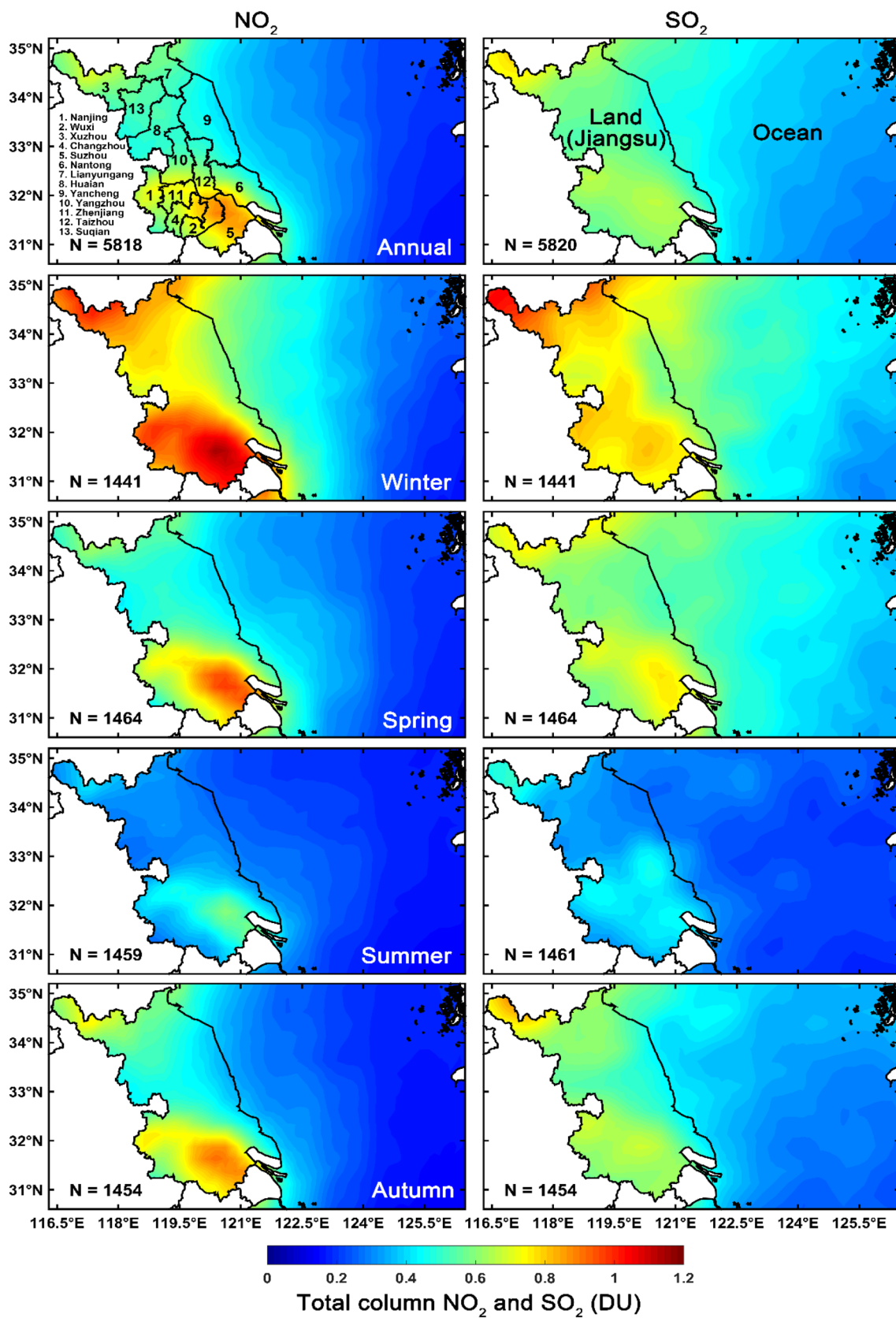
Fig. 2 Annual and spatial distribution of OMI-based NO$_2$ (DU) and SO$_2$ (DU) over ocean and land areas of Jiangsu Province, China, averaged for the period 2005 to 2020 [N defines the number of valid pixels]

Table 1 Annual and seasonal mean NO_2 and SO_2 ($\pm$ STD), obtained from OMI for the period 2005–2020 over ocean and land surfaces (Jiangsu Province)

	Trace gas	Ocean	Land
Annual	NO_2	0.30 ± 0.03	0.58 ± 0.06
	SO_2	0.38 ± 0.06	0.56 ± 0.11
Winter	NO_2	0.44 ± 0.08	0.83 ± 0.12
	SO_2	0.50 ± 0.09	0.75 ± 0.16
Spring	NO_2	0.29 ± 0.03	0.56 ± 0.08
	SO_2	0.44 ± 0.09	0.60 ± 0.15
Summer	NO_2	0.20 ± 0.01	0.34 ± 0.02
	SO_2	0.23 ± 0.03	0.33 ± 0.06
Autumn	NO_2	0.25 ± 0.03	0.58 ± 0.05
	SO_2	0.34 ± 0.05	0.54 ± 0.14

were highest at 0.60–0.75 bin, which is mainly attributed to more emission from heating, weak photochemical conversion, and atmospheric mixing (Qi et al. 2012). Over ocean surfaces, the NO_2 occurrence frequencies of 0.15–0.30 bin were highest in all seasons, while the SO_2 occurrence frequencies of 0.15–0.30 bin were highest in autumn and summer and the 0.30–0.45 bin in winter and spring (Fig. 3). This indicates that a moderate level of SO_2 pollution across ocean surfaces in winter and spring is mainly transported from land surfaces. Recent studies also reported that the winter and spring SO_2 pollution over ocean surfaces (including the Yellow Sea) primarily comes from Eastern China (Jeon et al. 2021, 2018).

4.3 OMI SO_2/ NO_2 ratio

The SO_2/NO_2 ratio was used to detect the sources of air pollutants over land, whether from mobile sources (traffic emissions) or point sources (industrial activities) (Abdul Halim et al. 2018; Aneja et al. 2001; Nirel and Dayan 2001; Wang et al. 2021b) and over the ocean from ship emissions (Cheng et al. 2019a; Zhou et al. 2019). The results show significant annual and seasonal variations in SO_2/NO_2 ratio over land and ocean (Fig. 4). Annually, the SO_2/NO_2 ratio over land varied from 1.28 to 1.36 during 2005–2008, indicating more SO_2 emissions than NO_2 from point sources. Over the ocean, the SO_2/NO_2 ratio ranged from 1.52 to 1.71 during the same period, indicating the emission of high-sulfur fuel content from Ships. Afterward, the ratio gradually drops from 2009 both over land (SO_2/NO_2: 0.76–0.96) and ocean (SO_2/NO_2: 1.02–1.24). The installation of the fuel gas desulfurization (FGD) device in the industry in 2007 (Zhang et al. 2017a, b) may reduce SO_2 emissions over land (Wang et al. 2021b). In addition, the International Maritime Organization and the Chinese Ministry of Transport (MOT) set up three domestic ship emission control areas in China (the Pearl River Delta: PRD, YRD, and the Bohai Rim: Beijing-Tianjin-Hebei area) where ship fuels were restricted to have a sulfur content of less than or equal to 0.50% (mass-by-mass) (MOT 2015). The 16-year area-averaged annual mean SO_2/NO_2 ratio was 1.27 across the ocean surface, reflecting emissions from ships using fuel with lower sulfur content. However, the ratio was 0.97 over land surfaces, indicating comparatively lower SO_2 emissions than NO_2 from point sources (e.g., industries)

Fig. 3 Annual and seasonal frequency distributions of OMI-based NO_2 and SO_2 (DU) over ocean and land areas of Jiangsu Province, China, for the period 2005–2020
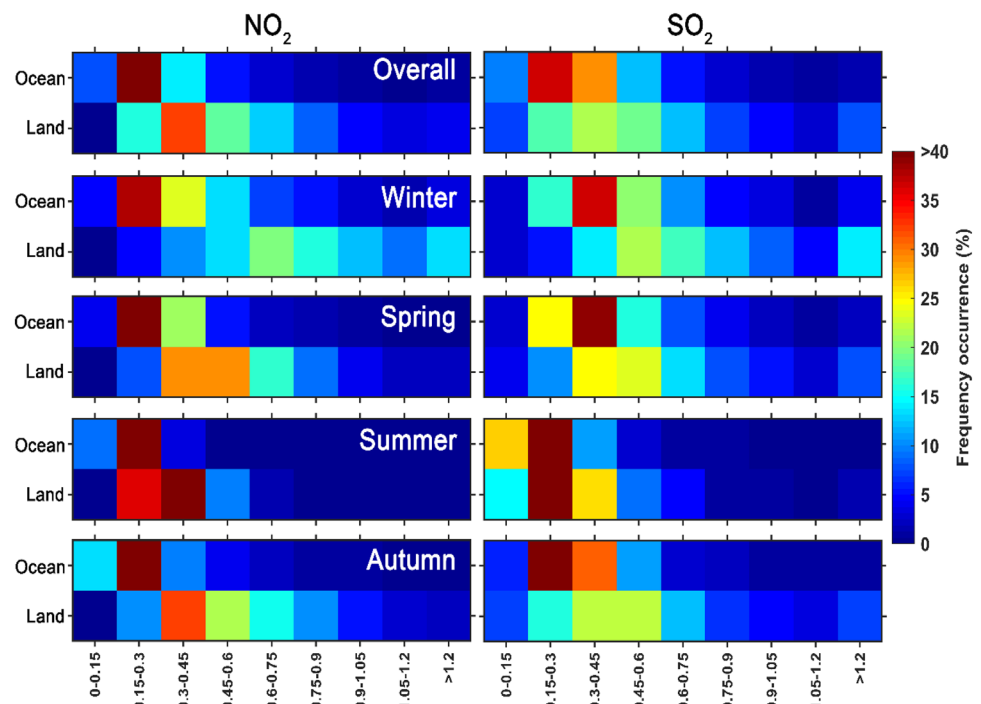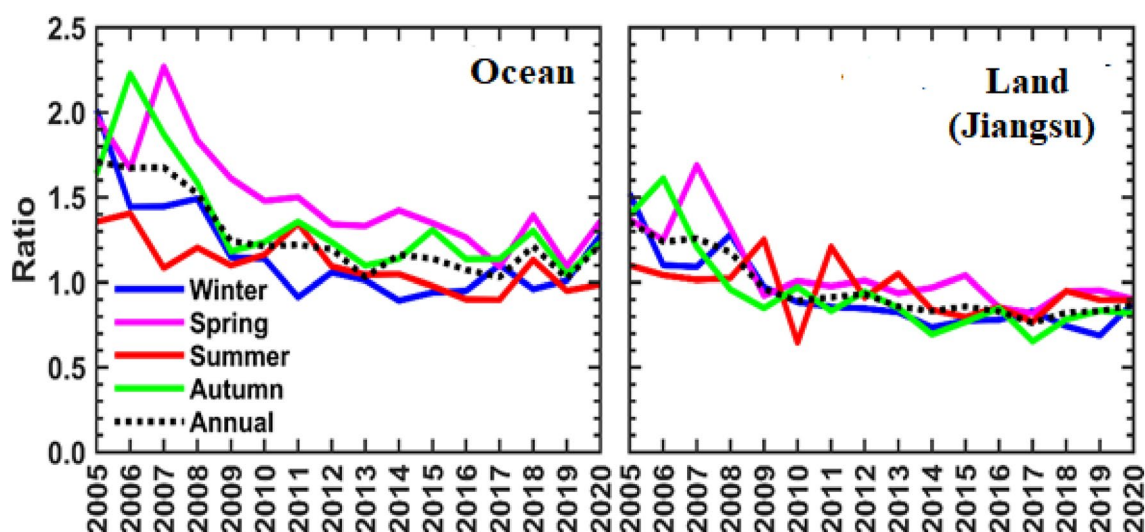
Fig. 4 Annual and seasonal variations of SO_2/NO_2 ratio obtained from OMI sensor for 2005–2020

(Table S1). Seasonally, high sulfur content emissions from ships were found in spring (SO_2/NO_2: 1.50) over the ocean surface, and lower sulfur content emissions from ships were prominent in summer (1.11) than in winter (1.18) and autumn (1.36). Over land, the SO_2/NO_2 ratio (1.06) in spring indicates that SO_2 emission was comparatively high than NO_2, while SO_2 emission was lower than NO_2 (Table S1) in summer (0.96), autumn (0.93), and winter (0.92) seasons (Table S1). These results signify that NO_2 and SO_2 emissions from point sources (industrial activities and ships) are responsible for polluting land and ocean surfaces. Recent studies reported that Ships have significant contributions to polluting land and ocean environments (Moldanová et al. 2022; Schwarzkopf et al. 2022; Zhai et al. 2023).

4.4 Spatio-Temporal Scenarios of Anthropogenic NO_x and SO_2 Emissions

Trace gases are those gases (e.g., carbon monoxide: CO, carbon dioxide: CO_2, Methane: CH_4, formaldehyde: HCHO, nitrogen species: NO_x, nitrous oxide: NO_2, sulfur dioxide: SO_2, and Ozone: O_3) that exist in the atmosphere which comes from biogenic processes, oceanic and anthropogenic emissions, and volcanoes, while anthropogenic emissions describe the gases and particles which comes from various sources (e.g., point sources and mobile sources). This section used the emission datasets to study the spatial and temporal distribution of NO_x and SO_2 emissions (Fig. 5). The spatial distributions of annual mean NO_x ($NO_x = NO_2 + NO$; 2007–2018) and SO_2 (2005–2014) emissions (unit: Giga gram or Gg) were higher over land than over the ocean (Fig. 5). The higher NO_x and SO_2 emissions in northern (Xuzhou, Suqian, and Lianyuang) and southern (Changzhou,

Nanjing, Suzhou, Wuxi, and Zhenjiang) cities of Jiangsu Province was consistent with OMI-based NO_2 and SO_2 measurements (Fig. 2). In particular, the area-averaged annual mean NO_x and SO_2 emissions were relatively high across the land (2.31 ± 0.20 for NO_x and 9.18 ± 1.57 for SO_2) in comparison with the ocean (0.43 ± 0.15 for NO_x) (Fig. 5), which can be attributed mainly to the higher level of anthropogenic activity over land. Furthermore, good correlation coefficients were found between OMI NO_2 and NO_x emission ($r = 0.626$) and OMI SO_2 vs. SO_2 emission ($r = 0.871$) over land surfaces. While lower correlation coefficient ($r = 0.366$) was found between OMI-NO_2 and NO_x emission over the ocean (Fig. 6). Previous studies reported that industrial anthropogenic activities are the major causes of higher NO_x and SO_2 emissions in China (Zheng et al. 2018a, b).

4.5 Trends of Satellite-Based and Emission-Based NO_2 and SO_2

The OMI NO_2 and SO_2 trends were calculated to assess annual and seasonal changes in NO_2 and SO_2 over land and ocean. Trends were calculated for 2005–2020 and 2006–2010, when China announced strict air pollution control policies during the 11th Five Year Plan (FYP) period, 2011–2015 (during the 12th FYP), and 2013–2017 (Action Plan of Air Pollution Prevention and Control: APPC-AC), as shown in Figs. 7, 8 and Table S2. The black dots (.) represents significant trends at a 95% confidence level. A clear spatial contrast in NO_2 and SO_2 trends was noticed during the study periods (Figs. 7 and 8). Notably, stronger decreasing trends in NO_2 and SO_2 concentrations were evident over land than over the ocean at annual and seasonal scales

Fig. 5 Spatial distributions of mean NO$_x$ (2007–2018) and SO$_2$ (2005–2014) emissions, estimated from OMI sensor, over China's ocean and land territories [Gg is for Giga gram]
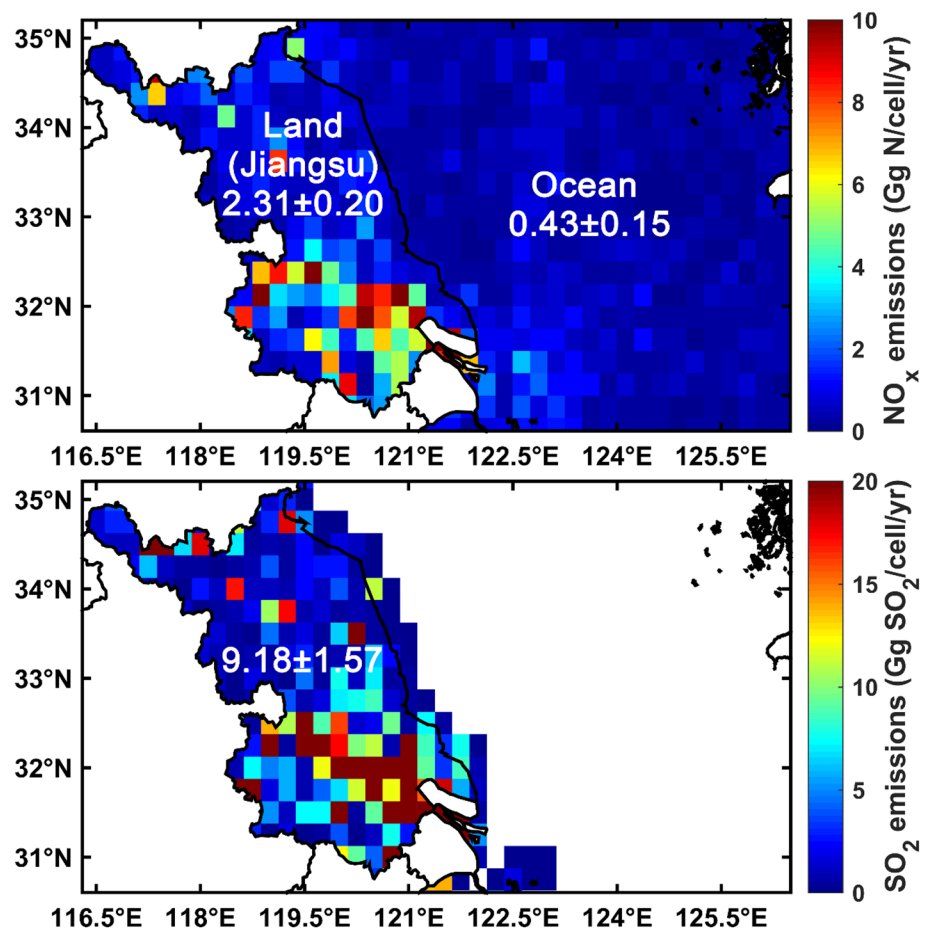
(Fig. 9 and Table S2). In particular, insignificant decreasing trends in annual NO$_2$ concentrations over land were higher in 2011–2015 (− 0.033/year) than in 2013–2017 (− 0.018/year), whereas the decreasing trends over the ocean were higher in 2011–2015 (− 0.014/year) than in 2013–2017 (− 0.001/year) (Fig. 9). In contrast, significant increasing trends in NO$_2$ were observed during the 11th Five Year Plan (FYP) period over land (2006–2010 = 0.023/year) and ocean (0.018/year). The stronger positive trends in 2006–2010 relative to the negative trends in 2011–2015 and 2013–2017 over the ocean led to an overall insignificant increasing trend in NO$_2$ (DU/year) in 2005–2020 (0.0004/year). The reverse scenarios were observed over land, leading to an insignificant decreasing trend in 2005–2020 (0.0004/year) (Fig. 9). Furthermore, significant decreasing trends in annual SO$_2$ were observed during 2005–2020 over land (− 0.023/year), which was higher than the ocean (− 0.011/year) (Fig. 9). Seasonally, significant decreasing trends in NO$_2$ and SO$_2$ (DU) were more prominent in 2005–2020 for all seasons than during other periods. Besides, the magnitudes of decreasing trends were higher over land than the ocean (Table S2). Several possible factors are responsible for the increasing and decreasing trends in NO$_2$ and SO$_2$ over land

and ocean. For example, desulfurization projects in coal-fired power plants were implemented during the 11th Five Year Plan (FYP) period (2006–2010) and continued for the 12th FYP period (2011–2015) and APPC-AC (2013–207) (Li et al. 2017a, b; Ma et al. 2019), which overall led to decreasing trends in SO$_2$ over land. In contrast, the absence of any control policies for reducing NO$_2$ emission during the 11th Five Year Plan (FYP) period (2006–2010) (Ma et al. 2019) allowed increased NO$_2$ concentrations during that period (see Figs. 7 and 9). A previous study also reported a significant reduction in CO$_2$, NO$_2$, and SO$_2$ emissions across China due to installing the combined cycle technology in industrial and coal-fired power plants (de Gouw et al. 2014). Implementing the ship emission control policy by the MOT in 2015 may also reduce SO$_2$ emissions over the ocean (MOT 2015).

Trends in NO$_x$ and SO$_2$ emissions were calculated to measure the relative contributions of anthropogenic NO$_x$ (Gg N/Cell/year) and SO$_2$ (Gg SO$_2$/Cell/year) emissions to OMI NO$_2$ and SO$_2$ changes. A large spatial contrast in NO$_x$ and SO$_2$ trends was observed during the study periods over the ocean and Jiangsu Province's land (Figs. S1, S2). A
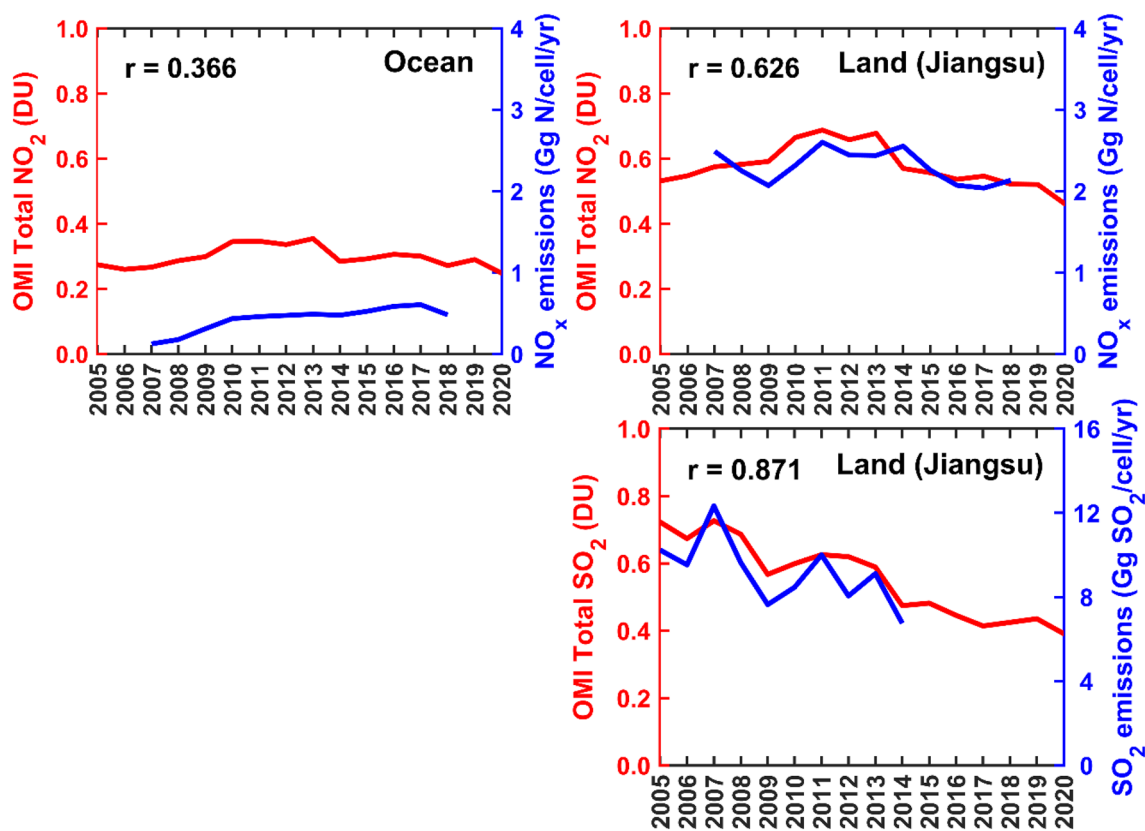
Fig. 6 The annual variability of OMI NO_2 and SO_2 emissions (NO_x and SO_2) over China's ocean and land surfaces

stronger positive trend in anthropogenic NO_x emission in 2007–2010 (0.114/year) than in 2013–2017 (0.036/year) or 2011–2015 (0.015/year) led to an overall significant increasing trend in 2007–2018 (0.032/year) over ocean. The positive trend signifies no significant control measurements of anthropogenic NO_x emission over ocean. Ships emit about $5–7 \times 10^9$ kg/year of NO_x and $4.7–6.5 \times 10^9$ kg/year of SO_2 into the atmosphere (Healy et al. 2009) and contribute to reducing air quality in both coastal and port cities (Andersson et al. 2009; Corbett et al. 1999; Endresen 2003). However, implementing China's strict air pollution control policies in high emitting sectors (e.g., industry, transport, and power plants) reduced anthropogenic NO_x and SO_2 emissions over land during the study periods (Fig. S2). This finding aligns with Zheng et al. (2018a, b) study. Overall, this study indicates that Chinese air pollution control policies contributed to improved air quality in Jiangsu by reducing NO_2 and SO_2. Therefore, these policies should be continued or extended in the future in order to improve

Chinese air quality, which will benefit the lives of citizens in the long run.

4.6 Potential Source Contribution Function (PSCF) analysis

The previous study reported that the air quality over land (i.e., Jiangsu Province) is significantly impacted more by local pollution than by distant regional sources (Fig. S3) (Wang et al. 2021b). In contrast, many industries are located in the land of Jiangsu province, especially in its southern cities, which may collectively contribute to forming high concentrations of NO_2 and SO_2 over those areas (Song et al. 2019). Therefore, PSCF analysis was conducted only over ocean for 2005–2020, using 72-h back trajectories attained from the NOAA HYSPLIT model and OMI data to detect the potential source areas of NO_2 and SO_2 pollutants. The HYSPLIT-derived back-trajectories from seven locations over ocean (see Table S3) were used to compute a single PSCF for each
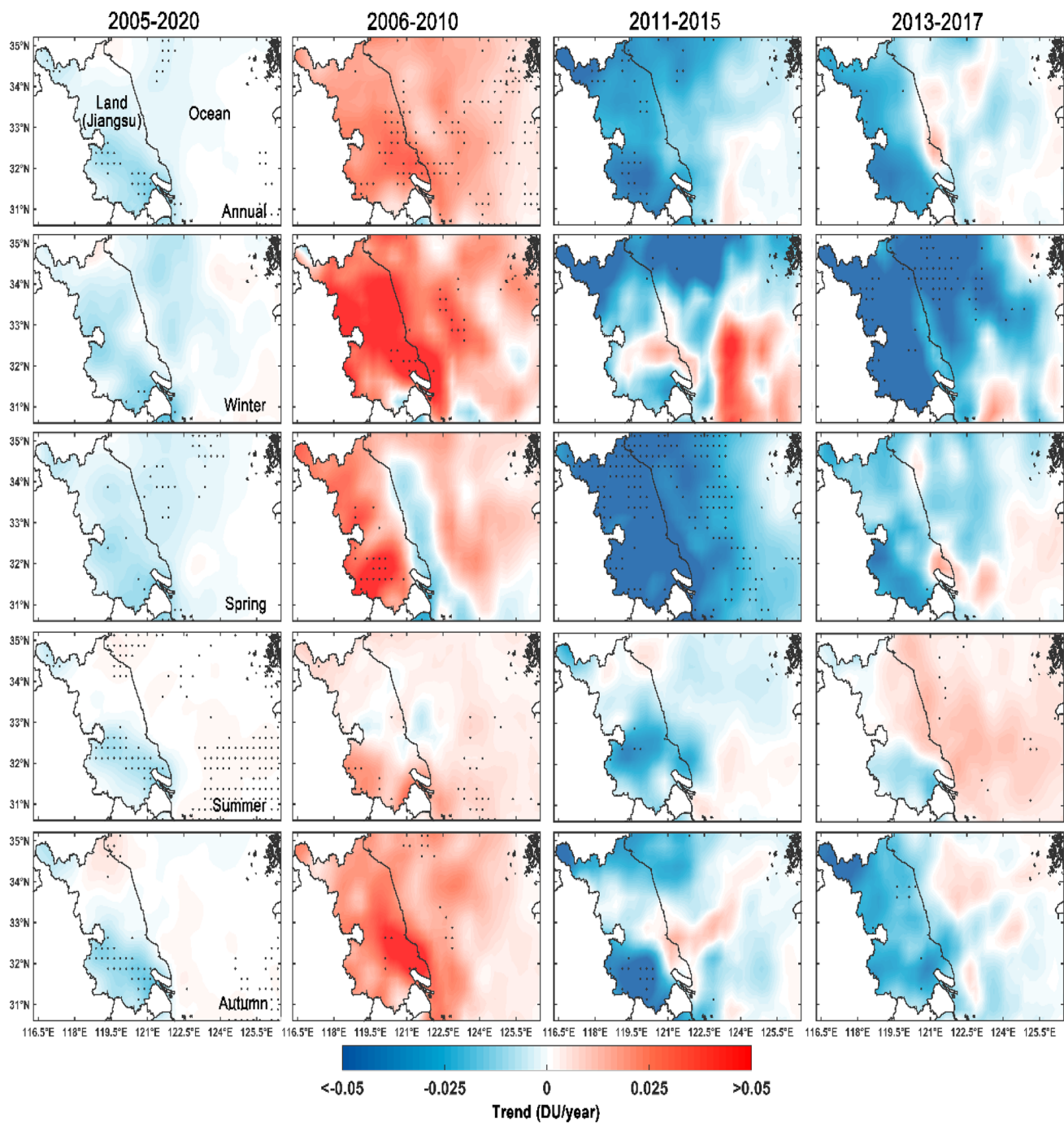
Fig. 7 Spatial distribution of annual and seasonal trends in OMI-based NO$_2$ concentrations. The black dot (.) indicates significance at a 95% confidence interval

air pollutant and show the major likely sources of pollution at those seven locations. PSCF analyses are grouped by season (Fig. 10). Significant seasonal variation in SO$_2$ and NO$_2$ sources was observed over the ocean. The high values of PSCF (> 0.50) in winter indicate that the potential source areas of NO$_2$ and SO$_2$ are located in different parts of mainland China (e.g., Anhui, Beijing, Henan, Hubei, Inner Mongolia, Jiangsu, Jiangxi, Shanxi,
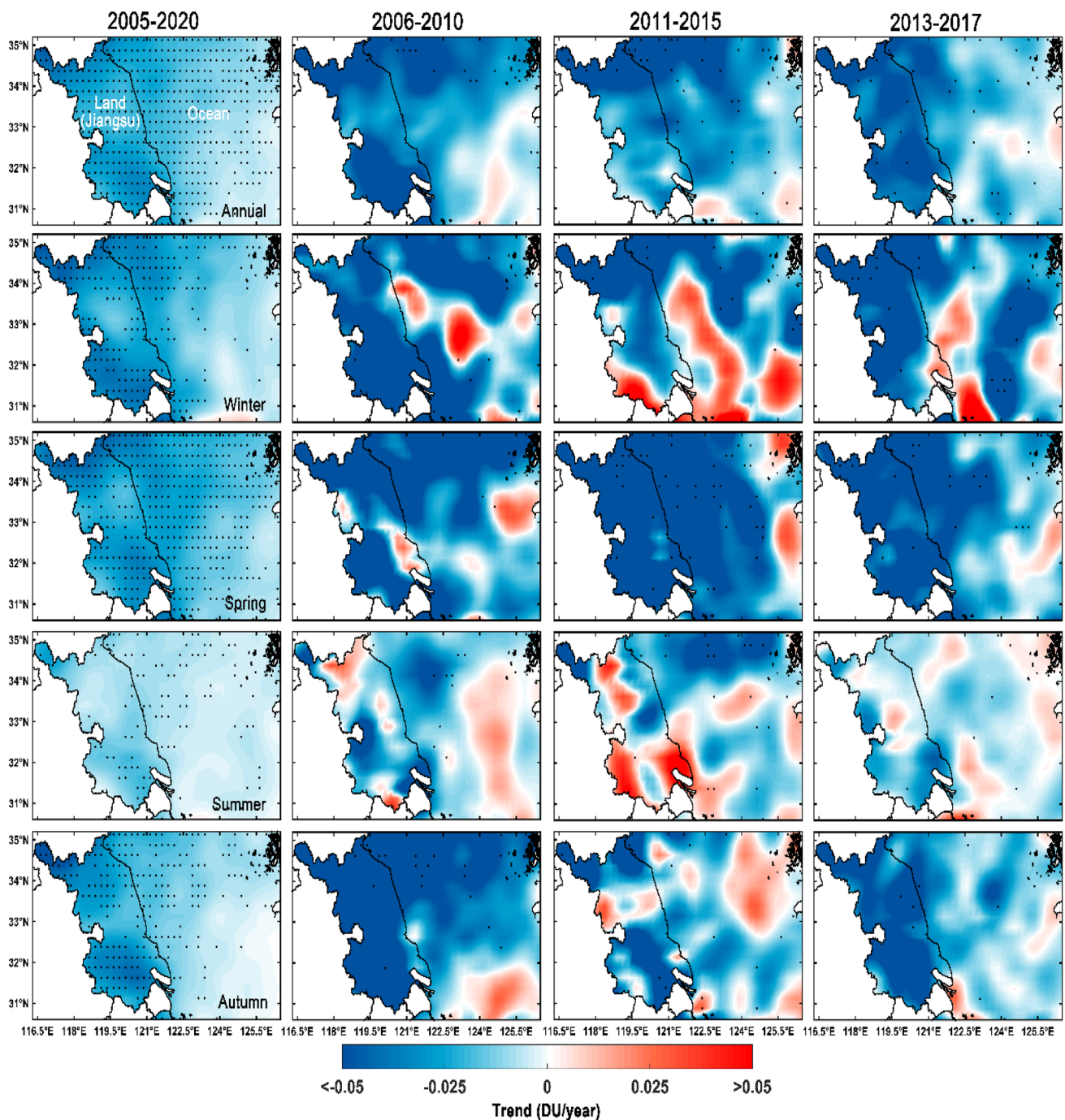
Fig. 8 Spatial distribution of annual and seasonal trends in OMI-based SO$_2$ concentrations. The black dot (.) symbol indicates significance at a 95% confidence interval

Shaanxi, Shandong, Tianjin, and Zhejiang). These local sources affect the air quality of ocean more significantly than the more distant regional sources (e.g., Mongolia) (Fig. 10). In spring, local sources (i.e., Anhui, Beijing, Henan, Hubei, Inner Mongolia, Jiangsu, Jiangxi, Shanxi, Shaanxi, Shandong, Tianjin, and Zhejiang) also substantially affect the air quality over ocean more than distant

regional sources like Mongolia do. Note that pollution levels are lower in summer than in winter and spring. In summer, the air quality over ocean is much more affected by local sources than by distant regional sources. The autumn air quality over ocean is also significantly impacted by local pollution sources. Overall, the results show that local sources from mainland China are the
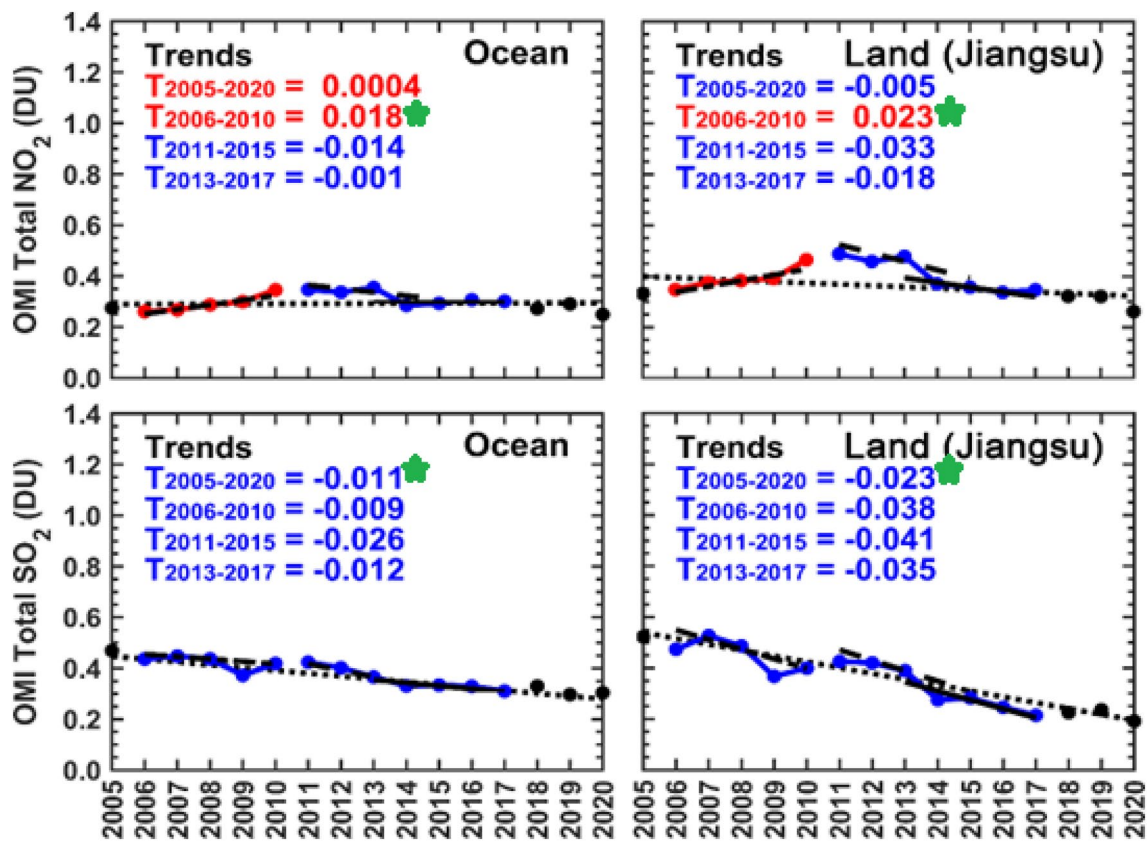
Fig. 9 Trends in OMI-based NO_2 and SO_2 for the periods 2005–2020, 2006–2010, 2011–2015, and 2013–2017 over ocean and land (Jiangsu Province). The red line indicates an increasing trend, and the blue line indicates a decreasing trend of NO_2 and SO_2. Asterisk (*) symbol indicates significance

major contributors to air pollution over land and ocean (Wang et al. 2021b), which are strongest in winter, followed by spring, autumn, and summer seasons.

5 Conclusions

The major findings are as follows:

- During the study period, NO_2 and SO_2 pollution hotspots were mainly located over land surfaces, which can be attributed to severe anthropogenic activities. On a seasonal scale, NO_2 and SO_2 were highest in winter and lowest in summer over land and ocean surfaces.
- The frequency distribution demonstrated that OMI NO_2 and SO_2 were higher over land than ocean. The occurrence frequencies of NO_2 and SO_2 for 0.15–0.30 bin

were common over ocean surfaces, and 0.30–0.45 bin was common across land surfaces.
- A good agreement was found between OMI NO_2 and SO_2 and anthropogenic emissions (NO_x and SO_2) across land surfaces than the ocean.
- Annually, OMI NO_2 (DU) over land surfaces showed insignificant decreasing trends from 2005 to 2020, while NO_2 (DU) over ocean surfaces showed minor increasing trends. Moreover, significant decreasing trends in SO_2 (DU) were larger over land surfaces than the ocean.
- Anthropogenic emissions of NO_x and SO_2 were decreased over land surfaces, while NOx emissions across ocean surfaces showed significant increasing trends.
- The PSCF analysis identified higher contributions of NO_2 and SO_2 over ocean and land from local sources than from long distant regional sources. These contributions are stronger in winter, followed by spring, autumn, and summer seasons.
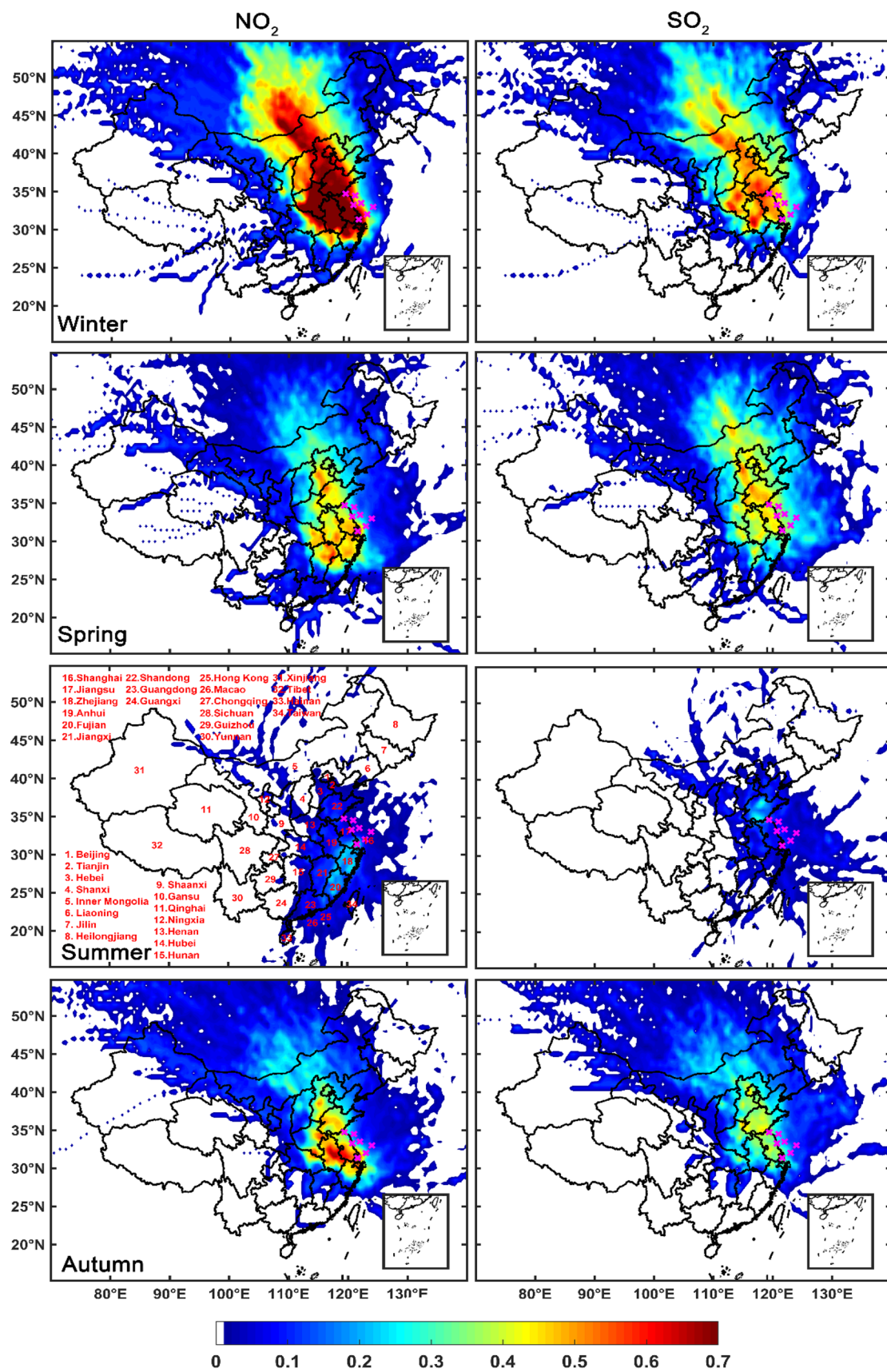
Fig. 10 Source identification of NO$_2$ and SO$_2$ over Ocean areas of Jiangsu Province in China during 2005–2020 using the PSCF at seasonal timescales

Data availability Data are available on request.

Declarations

Conflict of interest All authors declare that there is no conflict of interest.

References

Abdul Halim ND, Latif MT, Ahamad F, Dominick D, Chung JX, Juneng L, Khan MF (2018) The long-term assessment of air quality on an island in Malaysia. Heliyon 4:e01054. https://doi.org/10.1016/j.heliyon.2018.e01054

Ali MA, Huang Z, Bilal M, Assiri ME, Mhawish A, Nichol JE, de Leeuw G, Almazroui M, Wang Y, Alsubhi Y (2023) Long-term $PM_{2.5}$ pollution over China: identification of PM2.5 pollution hotspots and source contributions. Sci Total Environ 893:164871. https://doi.org/10.1016/j.scitotenv.2023.164871

Andersson C, Bergström R, Johansson C (2009) Population exposure and mortality due to regional background PM in Europe—long-term simulations of source region and shipping contributions. Atmos Environ 43:3614–3620. https://doi.org/10.1016/j.atmosenv.2009.03.040

Aneja VP, Agarwal A, Roelle PA, Phillips SB, Tong Q, Watkins N, Yablonsky R (2001) Measurements and analysis of criteria pollutants in New Delhi. India Environ Int 27:35–42. https://doi.org/10.1016/S0160-4120(01)00051-4

Berglen TF (2004) A global model of the coupled sulfur/oxidant chemistry in the troposphere: the sulfur cycle. J Geophys Res 109:D19310. https://doi.org/10.1029/2003JD003948

Bilal M, Mhawish A, Nichol JE, Qiu Z, Nazeer M, Ali MA, de Leeuw G, Levy RC, Wang Y, Chen Y, Wang L, Shi Y, Bleiweiss MP, Mazhar U, Atique L, Ke S (2021) Air pollution scenario over Pakistan: Characterization and ranking of extremely polluted cities using long-term concentrations of aerosols and trace gases. Remote Sens Environ 264:112617. https://doi.org/10.1016/j.rse.2021.112617

Boersma KF, Eskes HJ, Richter A, De Smedt I, Lorente A, Beirle S, van Geffen JHGM, Zara M, Peters E, Van Roozendael M, Wagner T, Maasakkers JD, van der ARJ, Nightingale J, De RudderA, Irie H, Pinardi G, Lambert JC, Compernolle SC, (2018) Improving algorithms and uncertainty estimates for satellite NO2 retrievals: Results from the Quality Assurance for Essential Climate Variables (QA4ECV) project. Atmos Meas Tech 11:6651–6678. https://doi.org/10.5194/amt-11-6651-2018

Bovensmann H, Burrows JP, Buchwitz M, Frerick J, Noël S, Rozanov VV, Chance KV, Goede APH (1999) SCIAMACHY: mission objectives and measurement modes. J Atmos Sci 56:127–150. https://doi.org/10.1175/1520-0469(1999)056%3c0127:SMOAMM%3e2.0.CO;2

Burrows JP, Weber M, Buchwitz M, Rozanov V, Ladstätter-Weißenmayer A, Richter A, DeBeek R, Hoogen R, Bramstedt K, Eichmann K-U, Eisinger M, Perner D (1999) The Global Ozone Monitoring Experiment (GOME): mission concept and first scientific results. J Atmos Sci 56:151–175. https://doi.org/10.1175/1520-0469(1999)056%3c0151:TGOMEG%3e2.0.CO;2

Callies J, Corpaccioli E, Eisinger M, Lefebvre A, Munro R, Perez-Albinana A, Ricciarelli B, Calamai L, Gironi G, Veratti R, Otter G, Eschen M, van Riel L (2004) GOME-2 ozone instrument onboard the European METOP satellites. In: Vonder Haar TH, Huang HLA (eds) Weather and environmental satellites. https://doi.org/10.1117/12.557860

Carey IM, Atkinson RW, Kent AJ, van Staa T, Cook DG, Anderson HR (2013) Mortality associations with long-term exposure to outdoor air pollution in a national english cohort. Am J Respir Crit Care Med 187:1226–1233. https://doi.org/10.1164/rccm.201210-1758OC

Celarier EA, Brinksma EJ, Gleason JF, Veefkind JP, Cede A, Herman JR, Ionov D, Goutail F, Pommereau JP, Lambert JC, van Roozendael M, Pinardi G, Wittrock F, Schönhardt A, Richter A, Ibrahim OW, Wagner T, Bojkov B, Mount G, Spinei E, Chen CM, Pongetti TJ, Sander SP, Bucsela EJ, Wenig MO, Swart DPJ, Volten H, Kroon M, Levelt PF (2008) Validation of ozone monitoring instrument nitrogen dioxide columns. J Geophys Res 113:D15S15. https://doi.org/10.1029/2007JD008908

Chan CK, Yao X (2008) Air pollution in mega cities in China. Atmos Environ 42:1–42. https://doi.org/10.1016/j.atmosenv.2007.09.003

Chen T, Deng S, Gao Y, Qu L, Li M, Chen D (2017) Characterization of air pollution in urban areas of Yangtze River Delta. China Chinese Geogr Sci 27:836–846. https://doi.org/10.1007/s11769-017-0900-z

Cheng Y, Wang S, Zhu J, Guo Y, Zhang R, Liu Y, Zhang Y, Yu Q, Ma W, Zhou B (2019a) Surveillance of SO_2 and NO_2 from ship emissions by MAX-DOAS measurements and implication to compliance of fuel sulfur content. Atmos Chem Phys 19:13611–13626. https://doi.org/10.5194/acp-2019-369

Cheng Y, Wang S, Zhu J, Guo Y, Zhang R, Liu Y, Zhang Y, Yu Q, Ma W, Zhou B (2019b) Surveillance of SO2 and NO2 from ship emissions by MAX-DOAS measurements and the implications regarding fuel sulfur content compliance. Atmos Chem Phys. https://doi.org/10.5194/acp-19-13611-2019

Corbett JJ, Fischbeck PS, Pandis SN (1999) Global nitrogen and sulfur inventories for oceangoing ships. J Geophys Res Atmos 104:3457–3470. https://doi.org/10.1029/1998JD100040

Cui Y, Lin J, Song C, Liu M, Yan Y, Xu Y, Huang B (2016) Rapid growth in nitrogen dioxide pollution over Western China, 2005–2013. Atmos Chem Phys 16:6207–6221. https://doi.org/10.5194/acp-16-6207-2016

Dahiya S, Myllyvirta L (2019) Global SO 2 emission hotspot database RANKING THE WORLD'S WORST SOURCES OF SO 2 POLLUTION Content

de Leeuw G, van der AR, Bai J, Xue Y, Varotsos C, Li Z, Fan C, Chen X, Christodoulakis I, Ding J, Hou X, Kouremadas G, Li D, Wang J, Zara M, Zhang K, Zhang Y (2021) Air quality over China. Remote Sens 13:3542. https://doi.org/10.3390/rs13173542

de Gouw JA, Parrish DD, Frost GJ, Trainer M (2014) Reduced emissions of CO_2, NO_x, and SO_2 from U.S. power plants owing to switch from coal to natural gas with combined cycle technology. Earth's Futur 2:75–82. https://doi.org/10.1002/2013EF000196

Ding J, van der ARJ, Mijling B, Jalkanen JP, Johansson L, Levelt PF (2018) Maritime NO_x emissions over Chinese seas derived from

satellite observations. Geophys Res Lett 45:2031–2037. https://doi.org/10.1002/2017GL076788

Ding J, van der ARJ, Mijling B, Levelt PF (2017) Space-based NOx emission estimates over remote regions improved in DECSO. Atmos Meas Tech 10:925–938. https://doi.org/10.5194/amt-10-925-2017

Ding J, Miyazaki K, van der ARJ, Mijling B, Kurokawa J, Cho S, Janssens-Maenhout G, Zhang Q, Liu F, Levelt PF (2017) Intercomparison of NOx emission inventories over East Asia. Atmos Chem Phys 17:10125–10141. https://doi.org/10.5194/acp-17-10125-2017

Dong G-H, Zhang P, Sun B, Zhang L, Chen X, Ma N, Yu F, Guo H, Huang H, Lee YL, Tang N, Chen J (2012) Long-term exposure to ambient air pollution and respiratory disease mortality in Shenyang, China: a 12-year population-based retrospective cohort study. Respiration 84:360–368. https://doi.org/10.1159/000332930

Eisinger M, Burrows JP (1998) Tropospheric sulfur dioxide observed by the ERS-2 GOME instrument. Geophys Res Lett 25:4177–4180. https://doi.org/10.1029/1998GL900128

Endresen Ø (2003) Emission from international sea transportation and environmental impact. J Geophys Res 108:4560. https://doi.org/10.1029/2002JD002898

Eyring V, Isaksen ISA, Berntsen T, Collins WJ, Corbett JJ, Endresen O, Grainger RG, Moldanova J, Schlager H, Stevenson DS (2010) Transport impacts on atmosphere and climate: Shipping. Atmos Environ 44:4735–4771. https://doi.org/10.1016/j.atmosenv.2009.04.059

Fan Q, Zhang Y, Ma W, Ma H, Feng J, Yu Q, Yang X, Ng SKW, Fu Q, Chen L (2016) Spatial and seasonal dynamics of ship emissions over the Yangtze River Delta and East China Sea and their potential environmental influence. Environ Sci Technol 50:1322–1329. https://doi.org/10.1021/acs.est.5b03965

Feng Z, Huang Y, Feng Y, Ogura N, Zhang F (2001) Chemical composition of precipitation in Beijing area, Northern China. Water Air Soil Pollut 125:345–356. https://doi.org/10.1023/A:1005287102786

Fleming ZL, Monks PS, Manning AJ (2012) Review: untangling the influence of air-mass history in interpreting observed atmospheric composition. Atmos Res 104–105:1–39. https://doi.org/10.1016/j.atmosres.2011.09.009

Healy RM, O'Connor IP, Hellebust S, Allanic A, Sodeau JR, Wenger JC (2009) Characterisation of single particles from in-port ship emissions. Atmos Environ 43:6408–6414. https://doi.org/10.1016/j.atmosenv.2009.07.039

Hilboll A, Richter A, Burrows JP (2013) Long-term changes of tropospheric NO_2 over megacities derived from multiple satellite instruments. Atmos Chem Phys 13:4145–4169. https://doi.org/10.5194/acp-13-4145-2013

Hutchinson TC, Whitby LM (1977) The effects of acid rainfall and heavy metal particulates on a boreal Forest ecosystem near the sudbury smelting region of Canada. Water Air Soil Pollut. https://doi.org/10.1007/BF00285542

Jain RK, Cui Z, Domen JK (2016) Environmental impacts of mining. In: Environmental impact of mining and mineral processing. Elsevier, New York, pp 53–157. https://doi.org/10.1016/B978-0-12-804040-9.00004-8

Jeon W, Choi Y, Mun J, Lee S-H, Choi H-J, Yoo J-W, Lee H-J, Lee HW (2018) Behavior of sulfate on the sea surface during its transport from Eastern China to South Korea. Atmos Environ 186:102–112. https://doi.org/10.1016/j.atmosenv.2018.05.017

Jeon W, Park J, Choi Y, Mun J, Kim D, Kim C-H, Lee H-J, Bak J, Jo H-Y (2021) The mechanism of the formation of high sulfate concentrations over the Yellow Sea during the KORUS-AQ period: the effect of transport/atmospheric chemistry and ocean

emissions. Atmos Res 261:105756. https://doi.org/10.1016/j.atmosres.2021.105756

Jion MMMF, Jannat JN, Mia MY et al (2023) A critical review and prospect of NO_2 and SO_2 pollution over Asia: hotspots, trends, and sources. Sci Total Environ 876:162851. https://doi.org/10.1016/j.scitotenv.2023.162851

Johansson L, Jalkanen J-P, Kukkonen J (2017) Global assessment of shipping emissions in 2015 on a high spatial and temporal resolution. Atmos Environ 167:403–415. https://doi.org/10.1016/j.atmosenv.2017.08.042

Kendall MG (1975) Rank correlation methods (4th edn.) Charles Griffin, San Francisco, London

Krotkov NA, McLinden CA, Li C, Lamsal LN, Celarier EA, Marchenko SV, Swartz WH, Bucsela EJ, Joiner J, Duncan BN, Boersma KF, Veefkind JP, Levelt PF, Fioletov VE, Dickerson RR, He H, Lu Z, Streets DG (2016) Aura OMI observations of regional SO_2 and NO_2 pollution changes from 2005 to 2015. Atmos Chem Phys 16:4605–4629. https://doi.org/10.5194/acp-16-4605-2016

Lamsal LN, Martin RV, Parrish DD, Krotkov NA (2013) Scaling relationship for NO_2 pollution and urban population size: a satellite perspective. Environ Sci Technol 47:7855–7861. https://doi.org/10.1021/es400744g

Lee DS, Köhler I, Grobler E, Rohrer F, Sausen R, Gallardo-Klenner L, Olivier JGJ, Dentener FJ, Bouwman AF (1997) Estimations of global no, emissions and their uncertainties. Atmos Environ 31:1735–1749. https://doi.org/10.1016/S1352-2310(96)00327-5

Lelieveld J, Dentener FJ (2000) What controls tropospheric Ozone? J Geophys Res Atmos 105:3531–3551. https://doi.org/10.1029/1999JD901011

Lelieveld J, Peters W, Dentener FJ, Krol MC (2002) Stability of tropospheric hydroxyl chemistry. J Geophys Res Atmos. https://doi.org/10.1029/2002JD002272

Levelt PF, Hilsenrath E, Leppelmeier GW, van den Oord GHJ, Bhartia PK, Tamminen J, de Haan JF, Veefkind JP (2006a) Science objectives of the ozone monitoring instrument. IEEE Trans Geosci Remote Sens 44:1199–1208. https://doi.org/10.1109/TGRS.2006.872336

Levelt PF, van den Oord GHJ, Dobber MR, Malkki A, Visser H, de Vries J, Stammes P, Lundell JOV, Saari H (2006b) The ozone monitoring instrument. IEEE Trans Geosci Remote Sens 44:1093–1101. https://doi.org/10.1109/TGRS.2006.872333

Levelt PF, Joiner J, Tamminen J, Veefkind JP, Bhartia PK, Stein Zweers DC, Duncan BN, Streets DG, Eskes H, van der AR, McLinden C, Fioletov V, Carn S, de Laat J, DeLand M, Marchenko S, McPeters R, Ziemke J, Fu D, Liu X, Pickering K, Apituley A, González Abad G, Arola A, Boersma F, Chan Miller C, Chance K, de Graaf M, Hakkarainen J, Hassinen S, Ialongo I, Kleipool Q, Krotkov N, Li C, Lamsal L, Newman P, Nowlan C, Suleiman R, Tilstra LG, Torres O, Wang H, Wargan K (2018) The Ozone Monitoring Instrument: overview of 14 years in space. Atmos Chem Phys 18:5699–5745. https://doi.org/10.5194/acp-18-5699-2018

Li C, Zhang Q, Krotkov NA, Streets DG, He K, Tsay S-C, Gleason JF (2010) Recent large reduction in sulfur dioxide emissions from Chinese power plants observed by the Ozone Monitoring Instrument. Geophys Res Lett. https://doi.org/10.1029/2010GL042594

Li C, McLinden C, Fioletov V, Krotkov N, Carn S, Joiner J, Streets D, He H, Ren X, Li Z, Dickerson RR (2017a) India is overtaking China as the world's largest emitter of anthropogenic sulfur dioxide. Sci Rep 7:14304. https://doi.org/10.1038/s41598-017-14639-8

Li M, Zhang Q, Kurokawa J, Woo J-H, He K, Lu Z, Ohara T, Song Y, Streets DG, Carmichael GR, Cheng Y, Hong C, Huo H, Jiang X, Kang S, Liu F, Su H, Zheng B (2017b) MIX: a mosaic Asian anthropogenic emission inventory under the international collaboration framework of the MICS-Asia and HTAP. Atmos Chem Phys 17:935–963. https://doi.org/10.5194/acp-17-935-2017

Lin J-T, McElroy MB (2011) Detection from space of a reduction in anthropogenic emissions of nitrogen oxides during the Chinese economic downturn. Atmos Chem Phys 11:8171–8188. https://doi.org/10.5194/acp-11-8171-2011

Liu F, Zhang Q, van der ARJ, Zheng B, Tong D, Yan L, Zheng Y, He K (2016) Recent reduction in NO_x emissions over China: synthesis of satellite observations and emission inventories. Environ Res Lett 11:114002. https://doi.org/10.1088/1748-9326/11/11/114002

Liu F, Beirle S, Zhang Q, van der ARJ, Zheng B, Tong D, He K (2017) NOx emission trends over Chinese cities estimated from OMI observations during 2005 to 2015. Atmos Chem Phys 17:9261–9275. https://doi.org/10.5194/acp-17-9261-2017

Lu Z, Streets DG, de Foy B, Krotkov NA (2013) Ozone monitoring instrument observations of interannual increases in SO_2 emissions from Indian coal-fired power plants during 2005–2012. Environ Sci Technol 47:13993–14000. https://doi.org/10.1021/es4039648

Lv Z, Liu H, Ying Q, Fu M, Meng Z, Wang Y, Wei W, Gong H, He K (2018) Impacts of shipping emissions on PM2.5 air pollution in China. Atmos Chem Phys 18:15811–15824. https://doi.org/10.5194/acp-18-15811-2018

Ma Z, Liu R, Liu Y, Bi J (2019) Effects of air pollution control policies on PM2.5 pollution improvement in China from 2005 to 2017: a satellite-based perspective. Atmos Chem Phys 19:6861–6877. https://doi.org/10.5194/acp-19-6861-2019

Mann HB (1945) Nonparametric TESTS AGAINST TREND. Econometrica 13:245. https://doi.org/10.2307/1907187

Matthias V, Bewersdorff I, Aulinger A, Quante M (2010) The contribution of ship emissions to air pollution in the North Sea regions. Environ Pollut 158:2241–2250. https://doi.org/10.1016/j.envpol.2010.02.013

Meng Z-Y, Xu X-B, Wang T, Zhang X-Y, Yu X-L, Wang S-F, Lin W-L, Chen Y-Z, Jiang Y-A, An X-Q (2010) Ambient sulfur dioxide, nitrogen dioxide, and ammonia at ten background and rural sites in China during 2007–2008. Atmos Environ 44:2625–2631. https://doi.org/10.1016/j.atmosenv.2010.04.008

Mhawish A, Banerjee T, Sorek-Hamer M, Bilal M, Lyapustin AI, Chatfield R, Broday DM (2020) Estimation of high-resolution PM 2.5 over the indo-gangetic plain by fusion of satellite data, meteorology, and land use variables. Environ Sci Technol 54:7891–7900. https://doi.org/10.1021/acs.est.0c01769

Mijling B, van der ARJ (2012) Using daily satellite observations to estimate emissions of short-lived air pollutants on a mesoscopic scale. J Geophys Res Atmos. https://doi.org/10.1029/2012JD017817

Miller BG (2005) The effect of coal usage on human health and the environment. In: Coal energy systems. Elsevier, New York, pp 77–122. https://doi.org/10.1016/B978-012497451-7/50003-6

Moldanová J, Hassellöv IM, Matthias V et al (2022) Framework for the environmental impact assessment of operational shipping. Ambio 51:754–769. https://doi.org/10.1007/s13280-021-01597-9

MOT (2015) MOT: implementation of the ship emission control area in Pearl River Delta, the Yangtze River Delta and the Bohai Rim (Beijing-Tianjin-Hebei area). http://www.chim-pn.com/Doc/implementation_plan_eng.pdf

Munro R, Lang R, Klaes D, Poli G, Retscher C, Lindstrot R, Huckle R, Lacan A, Grzegorski M, Holdak A, Kokhanovsky A, Livschitz J, Eisinger M (2016) The GOME-2 instrument on the Metop series of satellites: instrument design, calibration, and level 1 data processing—an overview. Atmos Meas Tech 9:1279–1301. https://doi.org/10.5194/amt-9-1279-2016

Nirel R, Dayan U (2001) On the ratio of sulfur dioxide to nitrogen oxides as an indicator of air pollution sources. J Appl Meteorol 40:1209–1222. https://doi.org/10.1175/1520-0450(2001)040%3c1209:OTROSD%3e2.0.CO;2

Penn E, Holloway T (2020) Evaluating current satellite capability to observe diurnal change in nitrogen oxides in preparation for geostationary satellite missions. Environ Res Lett 15:034038. https://doi.org/10.1088/1748-9326/ab6b36

Pope CA, Dockery DW (2006) Health effects of fine particulate air pollution: lines that connect. J Air Waste Manage Assoc 56:709–742. https://doi.org/10.1080/10473289.2006.10464485

Qi H, Lin W, Xu X, Yu X, Ma Q (2012) Significant downward trend of SO_2 observed from 2005 to 2010 at a background station in the Yangtze Delta region, China. Sci China Chem 55:1451–1458. https://doi.org/10.1007/s11426-012-4524-y

Schreier SF, Peters E, Richter A, Lampel J, Wittrock F, Burrows JP (2015) Ship-based MAX-DOAS measurements of tropospheric NO_2 and SO_2 in the South China and Sulu Sea. Atmos Environ 102:331–343. https://doi.org/10.1016/j.atmosenv.2014.12.015

Schwarzkopf DA, Petrik R, Matthias V, Quante M, Yu G, Zhang Y (2022) Comparison of the impact of ship emissions in northern Europe and eastern China. Atmosphere 13:894. https://doi.org/10.3390/atmos13060894

Seinfeld JH, Pandis SN (2006) Atmospheric chemistry and physics: from air pollution to climate change. In: Public administration review. Wiley, Hoboken

Sen PK (1968) Journal of the American statistical estimates of the regression coefficient based on Kendall's Tau. J Am Stat Assoc 63:1379–1389

Song C, Wu L, Xie Y, He J, Chen X, Wang T, Lin Y, Jin T, Wang A, Liu Y, Dai Q, Liu B, Wang Y, Mao H (2017) Air pollution in China: status and spatiotemporal variations. Environ Pollut 227:334–347. https://doi.org/10.1016/j.envpol.2017.04.075

Song R, Yang L, Liu M, Li C, Yang Y (2019) Spatiotemporal distribution of air pollution characteristics in Jiangsu Province. China Adv Meteorol 2019:1–14. https://doi.org/10.1155/2019/5907673

Stein AF, Draxler RR, Rolph GD, Stunder BJB, Cohen MD, Ngan F (2015) NOAA's HYSPLIT atmospheric transport and dispersion modeling system. Bull Am Meteorol Soc 96:2059–2077. https://doi.org/10.1175/BAMS-D-14-00110.1

Takashima H, Irie H, Kanaya Y, Syamsudin F (2012) NO_2 observations over the western Pacific and Indian Ocean by MAX-DOAS on *Kaiyo* a Japanese research vessel. Atmos Meas Tech 5:2351–2360. https://doi.org/10.5194/amt-5-2351-2012

Tan W, Liu C, Wang S, Xing C, Su W, Zhang C, Xia C, Liu H, Cai Z, Liu J (2018) Tropospheric NO2, SO2, and HCHO over the East China Sea, using ship-based MAX-DOAS observations and comparison with OMI and OMPS satellite data. Atmos Chem Phys 18:15387–15402. https://doi.org/10.5194/acp-18-15387-2018

Tao Y, Huang W, Huang X, Zhong L, Lu SE, Li Y, Dai L, Zhang Y, Zhu T (2012) Estimated acute effects of ambient Ozone and nitrogen dioxide on mortality in the Pearl River Delta of southern China. Environ Health Perspect. https://doi.org/10.1289/ehp.1103715

Theil H (1992) A rank-invariant method of linear and polynomial regression analysis BT—Henri Theil's contributions to economics and econometrics: econometric theory and methodology. Springer, Netherlands, pp 345–381

Theys N, De Smedt I, van Gent J, Danckaert T, Wang T, Hendrick F, Stavrakou T, Bauduin S, Clarisse L, Li C, Krotkov N, Yu H, Brenot H, Van Roozendael M (2015) Sulphur dioxide vertical column DOAS retrievals from the Ozone Monitoring Instrument: global observations and comparison to groundbased and satellite data. J Geophys Res Atmos 120:2470–2491. https://doi.org/10.1002/2014JD022657

van der ARJ, Mijling B, Ding J, Koukouli ME, Liu F, Li Q, Mao H, Theys N (2017) Cleaning up the air: Effectiveness of air quality policy for SO_2 and NO_x emissions in China. Atmos Chem Phys 17:1775–1789. https://doi.org/10.5194/acp-17-1775-2017

Veefkind JP, Aben I, McMullan K, Förster H, de Vries J, Otter G, Claas J, Eskes HJ, de Haan JF, Kleipool Q, van Weele M, Hasekamp O, Hoogeveen R, Landgraf J, Snel R, Tol P, Ingmann P, Voors R, Kruizinga B, Vink R, Visser H, Levelt PF (2012) TROPOMI on the ESA Sentinel-5 Precursor: a GMES mission for global observations of the atmospheric composition for climate, air quality and ozone layer applications. Remote Sens Environ 120:70–83. https://doi.org/10.1016/j.rse.2011.09.027

Wang S, Xing J, Chatani S, Hao J, Klimont Z, Cofala J, Amann M (2011) Verification of anthropogenic emissions of China by satellite and ground observations. Atmos Environ 45:6347–6358. https://doi.org/10.1016/j.atmosenv.2011.08.054

Wang Y, Beirle S, Lampel J, Koukouli M, De Smedt I, Theys N, Li A, Wu D, Xie P, Liu C, Van Roozendael M, Stavrakou T, Müller J-F, Wagner T (2017) Validation of OMI, GOME-2A and GOME-2B tropospheric NO_2 SO_2 and HCHO products using MAX-DOAS observations from 2011 to 2014 in Wuxi, China: investigation of the effects of prio. Atmos Chem Phys 17:5007–5033. https://doi.org/10.5194/acp-17-5007-2017

Wang Y, Ali MA, Bilal M, Qiu Z, Ke S, Almazroui M, Islam MM, Zhang Y (2021a) Identification of aerosol pollution hotspots in Jiangsu Province of China. Remote Sens 13:2842. https://doi.org/10.3390/rs13142842

Wang Y, Ali MA, Bilal M, Qiu Z, Mhawish A, Almazroui M, Shahid S, Islam MN, Zhang Y, Haque MN (2021b) Identification of NO_2 and SO_2 pollution hotspots and sources in Jiangsu Province of China. Remote Sens 13:3742. https://doi.org/10.3390/rs13183742

Wei J, Li Z, Wang J, Li C, Gupta P, Cribb M (2023) Ground-level gaseous pollutants (NO2, SO2, and CO) in China: daily seamless mapping and spatiotemporal variations. Atmos Chem Phys 23:1511–1532. https://doi.org/10.5194/acp-23-1511-2023,2023

Xue R, Wang S, Li D, Zou Z, Chan KL, Valks P, Saiz-Lopez A, Zhou B (2020) Spatio-temporal variations in NO2 and SO2 over Shanghai and Chongming Eco-Island measured by Ozone Monitoring Instrument (OMI) during 2008–2017. J Clean Prod 258:120563. https://doi.org/10.1016/j.jclepro.2020.120563

Zhai J, Yu G, Zhang J, Shi S, Yuan Y et al (2023) Impact of ship emissions on air quality in the greater bay area in china under the latest global marine fuel regulation. Environ Sci Technol 57(33):12341–12350. https://doi.org/10.1021/acs.est.3c03950

Zhang L, Jacob DJ, Boersma KF, Jaffe DA, Olson JR, Bowman KW, Worden JR, Thompson AM, Avery MA, Cohen RC, Dibb JE, Flock FM, Fuelberg HE, Huey LG, McMillan WW, Singh HB, Weinheimer AJ (2008) Transpacific transport of ozone pollution and the effect of recent Asian emission increases on air quality in North America: an integrated analysis using satellite, aircraft, ozonesonde, and surface observations. Atmos Chem Phys 8:6117–6136. https://doi.org/10.5194/acp-8-6117-2008

Zhang L, Lee CS, Zhang R, Chen L (2017a) Spatial and temporal evaluation of long term trend (2005–2014) of OMI retrieved NO_2 and SO_2 concentrations in Henan Province. China Atmos Environ 154:151–166. https://doi.org/10.1016/j.atmosenv.2016.11.067

Zhang Y, Yang X, Brown R, Yang L, Morawska L, Ristovski Z, Fu Q, Huang C (2017b) Shipping emissions and their impacts on air quality in China. Sci Total Environ 581–582:186–198. https://doi.org/10.1016/j.scitotenv.2016.12.098

Zheng F, Yu T, Cheng T, Gu X, Guo H (2014) Intercomparison of tropospheric nitrogen dioxide retrieved from Ozone Monitoring Instrument over China. Atmos Pollut Res 5:686–695. https://doi.org/10.5094/APR.2014.078

Zheng B, Tong D, Li M, Liu F, Hong C, Geng G, Li H, Li X, Peng L, Qi J, Yan L, Zhang Y, Zhao H, Zheng Y, He K, Zhang Q (2018a) Trends in China's anthropogenic emissions since 2010 as the consequence of clean air actions. Atmos Chem Phys 18:14095–14111. https://doi.org/10.5194/acp-18-14095-2018

Zheng C, Zhao C, Li Y, Wu X, Zhang K, Gao J, Qiao Q, Ren Y, Zhang X, Chai F (2018b) Spatial and temporal distribution of NO_2 and SO_2 in Inner Mongolia urban agglomeration obtained from satellite remote sensing and ground observations. Atmos Environ 188:50–59. https://doi.org/10.1016/j.atmosenv.2018.06.029

Zhou F, Gu J, Chen W, Ni X (2019) Measurement of SO_2 and NO_2 in Ship Plumes Using Rotary Unmanned Aerial System. Atmosphere (Basel) 10:657. https://doi.org/10.3390/atmos10110657

Authors and Affiliations

Md. Arfan Ali[1,2] (ORCID) **· Yu Wang[3] · Muhammad Bilal[4] · Mazen E. Assiri[2] · Abu Reza Md Towfiqul Islam[5,6] · Guilherme Malafaia[7,8,9] · Zhongwei Huang[1] · Alaa Mhawish[10] · M. Nazrul Islam[2] · Zhongfeng Qiu[3] · Rayees Ahmed[11] · Mansour Almazroui[12,13]**

✉ Zhongwei Huang
huangzhongwei@lzu.edu.cn

[1] Collaborative Innovation Center for West Ecological Safety (CIWES), Key Laboratory for Semi-Arid Climate Change of the Ministry of Education, College of Atmospheric Sciences, Lanzhou University, Lanzhou 730000, China

[2] The Climate Change Center at National Center for Meteorology, 21431 Jeddah, Saudi Arabia

[3] School of Marine Sciences, Nanjing University of Information Science & Technology, Nanjing 210044, China

[4] Center for Sustainability and the Global Environment (SAGE), Nelson Institute for Environmental Studies, University of Wisconsin—Madison, Madison, WI, USA

[5] Department of Disaster Management, Begum Rokeya University, Rangpur 5400, Bangladesh

[6] Department of Development Studies, Daffodil International University, Dhaka 1216, Bangladesh

[7] Post-Graduation Program in Conservation of Cerrado Natural Resources, Goiano Federal Institute, Urutaí, GO, Brazil

[8] Post-Graduation Program in Ecology, Conservation, and Biodiversity, Federal University of Uberlândia, Uberlândia, MG, Brazil

9   Post-Graduation Program in Biotechnology and Biodiversity, Federal University of Goiás, Goiânia, GO, Brazil

10   Sand and Dust Storm Warning Regional Center, National Center for Meteorology, 21431 Jeddah, Saudi Arabia

11   Department of Geography and Disaster Management, University of Kashmir, Srinagar 190006, India

12   Center of Excellence for Climate Change Research/Department of Meteorology, King Abdulaziz University, 21589 Jeddah, Saudi Arabia

13   Climatic Research Unit, School of Environmental Sciences, University of East Anglia, Norwich NR4 7TJ, UK